There is still some mystery as to how the ridge causes a hydraulic transition. When a subcritical flow encounters the ambient potential vorticity gradient is increased, which would seem to favor upstream propagation and thus even more supercritical flow. However, we are dealing with a varicose mode, whose properties are less well known. It might be a good idea to have a look at the Pratt and Pedlosky paper to see what the phase speed of a variscose wave is and how it depends on the pv change a-c.

6.4 A mid-latitude jet.

Unfortunately, global self-similarity is lost when the jet of the previous section is moved off of the equator ($f_o \neq 0$). Formulation of a hydraulic model of mid-latitude jet is possible but benefits from some further simplification. It will be helpful to work within the confines of the quasigeostrophic approximation, for which the layer depth is nearly constant and the Rossby number is small. In addition, it will be necessary to consider a special potential vorticity distribution.

We consider the reduced gravity, quasigeostrophic model as applied to a deep layer that flows along the bottom and is separated from the inactive upper layer by an interface. As discussed in Section 6.1, the interface displacement $\eta^{(0)}$ acts as a streamfunction ψ for the geostrophic velocity. For steady flow, the long-wave approximation to the quasigeostrophic potential vorticity (see 6.1.6) is

$$\frac{\partial^2 \psi}{\partial y^2} - S\psi + h + \beta y = q(\psi) \qquad (6.4.1)$$

The topography again consists of an isolated ridge but, unlike the previous example, y-variations in the height of the ridge will be key to hydraulic transitions in the overlying jet. We therefore set $h = \mathcal{N}(x)H(y)$.

The form of the potential vorticity function $q(\psi)$ can be constrained by considering a hypothetical upstream flow consisting of a jet that is centered near y=0 and that impinges of the ridge from the west. Far to the north and south of the jet, but still upstream, the flow is assumed to be westward and very broad: u=-u_o<0, where u_o is a constant. Evaluating (6.4.1) in these outer regions leads to $\beta y = q(\psi) + S\psi$ or, after differentiation with respect to y, $q'(\psi) = (\beta / u_o) - S$. The corresponding potential vorticity distribution is

$$q(\psi) = [(\beta / u_o) - S]\psi + const.. \qquad (6.4.2)$$

(The integration constant merely defines the reference value of ψ and has been set to zero.) It is expected that this distribution will be carried forward in x across the topography and therefore serve as a far field potential vorticity for the jet at all x.

The choice of $q(\psi)$ within the core of the jet can be motivated by noting that zonal currents like the Gulf Stream east of Cape Hatteras and the Jet Stream possess intrinsic potential vorticity gradients much stronger than β. These local gradients will be represented here by discontinuities in the value of q across certain streamlines. Specifically:

$$q(\psi) = [(\beta / u_o) - S]\psi + \hat{\delta}[y; L_1(x), L_2(x)] \tag{6.4.3}$$

where

$$\hat{\delta} = \begin{cases} a & y > L_1(x) \\ b & L_2(x) < y < L_1(x) \\ c & y < L_2(x) \end{cases}.$$

The flow is thus divided into three regions (I, II, and III), each containing the same potential vorticity gradient ($dq/d\psi$) but each having a different 'background' potential vorticity a, b, or c (Figure 6.4.1). The regions are separated by potential vorticity fronts coinciding with the streamlines at $y=L_1(x)$ and $y=L_2(x)$ across which $q(\psi)$ is discontinuous but velocity and ψ are continuous.

The potential vorticity equation (6.4.1) now becomes

$$\frac{\partial^2 \psi}{\partial y^2} - \alpha^2 \psi = -\beta y - \mathcal{N}(x) H(y) + \hat{\delta}[y; L_1(x), L_2(x)], \tag{6.4.4}$$

where $\alpha^2 = \beta / u_o$. The solution to (6.4.4) satisfying the condition of velocity continuity across the potential vorticity fronts and for which $\partial \psi / \partial y$ remains bounded as $y \to \pm\infty$ is

$$\psi = \begin{cases} (2\alpha^2)^{-1}[(b-c)e^{-\alpha \Delta L} + (a-b)]e^{-\alpha(y-L_1)} + \alpha^{-2}[\beta y + \mathcal{N}K - a] & (y > L_1) \\ (2\alpha^2)^{-1}[(b-a)e^{-\alpha(L_1-y)} + (b-c)e^{-\alpha(y-L_2)}] + \alpha^{-2}[\beta y + \mathcal{N}K - b] & (L_2 < y < L_1) \\ (2\alpha^2)^{-1}[(b-a)e^{-\alpha \Delta L} + (c-b)]e^{-\alpha(L_2-y)} + \alpha^{-2}[\beta y + \mathcal{N}K - c] & (y < L_2) \end{cases} \tag{6.4.5}$$

where $\Delta L = L_1 - L_2$ where $K(y)$ is a solution to

$$\frac{\partial^2 K}{\partial y^2} - \alpha^2 K = -\alpha^2 H(y). \tag{6.4.6}$$

The corresponding zonal velocity

$$u^{(o)} = -\frac{\partial \psi}{\partial y} = (2\alpha)^{-1}[(a-b)e^{-\alpha|y-L_1|} + (b-c)e^{-\alpha|y-L_2|}] - u_o - \alpha^{-2}\mathcal{N}\frac{dK}{dy} \qquad (6.4.7)$$

consists of the sum of the ambient westward velocity u_o, a topographic contribution related to dH/dy, and a pair of eastward cusped velocity profiles centered on the potential vorticity fronts (Figure 6.3.2). The scale $\alpha^{-1}=(u_o/\beta)^{1/2}$ is the distance over which the jet velocity decays away from a front.[1] It is now clear that the meridional isolation of the jet requires westward far-field flow. (An eastward far field ($u_o<0$) would yield a velocity profile with sinusoidal variations in y.)

The volume transport in core region (II) of the jet is

$$Q_2 = \int_{L_1}^{L_2} u dy = \alpha^{-2}\{\tfrac{1}{2}(a-c)(1-e^{-\alpha\Delta L}) - \beta\Delta L - \mathcal{N}[K(L_1)-K(L_2)]\}. \qquad (6.4.8)$$

If the elevation of the ridge increases linearly with y ($H = H_o + sy$, say) then the solution to (6.4.6) is $K(y) = H_o + sy$ and substitution into (6.4.8) leads to a relation between $\Delta L(x)$ and $\mathcal{N}$:

$$\mathcal{G}(\Delta L, \mathcal{N}) = s\mathcal{N} - \frac{\tfrac{1}{2}(a-c)(1-e^{-\alpha\Delta L}) - \beta\Delta L - \alpha^2 Q_2}{\Delta L} = 0 \qquad (6.4.9)$$

Note that ΔL depends only the potential vorticity difference a-c across the core and not on the potential vorticity b in the core itself.

Critical flow occurs for $\partial\mathcal{G}/\partial\Delta L = 0$, or

$$\frac{2\alpha^2 Q}{(a-c)} = 1 - (1+\alpha\Delta L)e^{-\alpha\Delta L}. \qquad (6.4.10)$$

The right-hand side increases monotonically from zero to unity as ΔL increases from zero to infinity. A critical state can therefore be found if and only if

$$0 \le \frac{2\alpha^2 Q}{(a-c)} \le 1. \qquad (6.4.11)$$

The numerator of this expression is proportional to $\beta Q/u_o$, the change in the planetary potential vorticity βy that would occur if the velocity had the uniform value u_o in the core. The denominator is clearly the change across the core of the potential vorticity intrinsic to

[1] This scale is also the boundary layer thickness in inertial models of basin circulations (Fofonoff, 1954) and of the Gulf Stream (Charney, 1955).

the flow. For critical flow to occur, the former must be weaker than the latter. In addition, the transport Q must have the same sign as a-c. To an observer facing downstream, the intrinsic potential vorticity must increase from right to left, meaning that the associated waves should tend to propagate upstream. We continue to assume that the jet is eastward (Q>0) so that a-c>0.

The topographic slope at the critical section can be found from substitution of (6.4.10) into (6.4.9). The resulting relation

$$\frac{2(\beta + s\mathcal{N}_c)}{\alpha(a-c)} = e^{-\alpha\Delta L_c} \tag{6.4.12}$$

forms the basis of a Froude number

$$F_\beta = \frac{\alpha(a-c)}{2(\beta + s\mathcal{N}_c)e^{\alpha\Delta L_c}}, \tag{6.4.13a}$$

such that F_β>1, <1, =1 for supercritical, subcritical and critical flow. A physical interpretation of the Froude number is aided by associating with the potential vorticity difference a-c an equivalent stream function difference $-\alpha^2(\psi_a - \psi_c)$, as suggested by (6.4.4). The difference $(\psi_c - \psi_a)$ is equal to the geostrophic flux Q_{ab} between two hypothetical regions with constant interface elevations a/α^2 and c/α^2. In addition, $\beta + s\mathcal{N}_c$ can be interpreted as the total ambient (planetary plus topographic) potential vorticity gradient: β_T, say. With these substitutions, the Froude number can be expressed using dimensional quantities as

$$F_\beta = \frac{Q_{ab}^*}{2\beta_T^* D L_\beta^3 e^{\Delta L^*/L_\beta}} \tag{6.4.13b}$$

where $L_\beta = (u_o^*/\beta^*)^{1/2}$. The term $Q_{ab}^*/\beta_T^* D L_\beta^3$ is similar to the familiar scale $U/\beta^* L^2$, with the total ambient potential vorticity gradient substituted for β^*, the inertial boundary layer thickness substituted for L, and the velocity scale Q_{ab}^*/DL_β used for U. If the ratio $\Delta L^*/L_\beta$ is not much larger than unity, meaning that the two fronts are separated by a single inertial radii or less, then flow criticality requires this particular version of $U/\beta^* L^2$ to be O(1) as well. On of the other hand, separation of the fronts by more than a few values of L_β means that the exponential term in (6.4.13b) becomes very large and thus a large potential vorticity difference a-c (and equivalent geostrophic flow) is required for critical control. The interpretation of this limit is that the two fronts lose their awareness of each other and become independent as they separate. Contact between the two can then be maintained only if the potential vorticity difference a-b, and thus the associated transport Q_{ac} is very large.

It follows from (6.4.9) that $\lim_{\Delta L\to\infty} s\mathcal{N} = -\beta$ whereas $\lim_{\Delta L\to 0} s\mathcal{N} = -\infty$,

both limits being evident in the Figure 6.4.2 plot of $s\mathcal{N}$ vs. ΔL. The curve has a maximum value for finite ΔL provided (6.4.11) is satisfied. Flows lying to the right are presumably subcritical and those to the left supercritical. Since the upstream and downstream states correspond to $s\mathcal{N}$=0, it is necessary that the maximum of the curve lie above the $s\mathcal{N}$ axis. Therefore a requirement for the existence of solutions, controlled or otherwise, is that $s\mathcal{N}_c$ is ≥0. Thus the ridge crest must slope upwards in the positive y direction.

For a given topographic function $s\mathcal{N}(x)$ it is possible to find the corresponding jet width $\Delta L(x)$ by tracing along the solution curve in Figure 6.4.2. It still remains to determine the individual latitudes of the potential vorticity fronts $y=L_2(x)$ and $y=L_2(x)+\Delta L(x)$. The former can be found through evaluation of (6.4.5) along the streamline $y=L_2(x)$, resulting in

$$L_2(x) = (\beta + \mathcal{N}s^{-1})[\beta L_2(-\infty) - \mathcal{N}H_o + \tfrac{1}{2}(a-b)(e^{-\alpha\Delta L} - e^{-\alpha\Delta L(-\infty)})]. \qquad (6.4.14)$$

Examples of the four standard hydraulic solutions (Figure 6.4.3) have been calculated from (6.4.9) and (6.4.14) for parameter settings close to those of Figure 6.4.2 and for $\mathcal{N}(x) = \mathcal{N}_{\max} e^{-x^2}$. The purely subcritical and supercritical solutions are distinguished by a narrowing or widening over the ridge. The subcritical-to-supercritical solution narrows as it passes the ridge and becomes supercritical, whereas the (unstable) supercritical-to-subcritical solution does the opposite.

If the ridge slopes southwards (s<0) rather than northwards and the upstream flow is subcritical, the solution over the ridge lies to the right of ΔL_u along the Figure 6.4.2 curve. As the subcritical jet climbs the topography its width increases and the flow becomes more subcritical. If $s\mathcal{N}_{\max} < -\beta$, ΔL becomes infinite before the ridge crest is reached. Although long-wave assumption becomes violated here there is a suggestion that the flow may become completely blocked by the ridge through deflection to the north and south.

In the ocean, a possible application of the above theory is to the Antarctic Circumpolar Current (ACC) as it passes over the Kerguelen Plateau or through the Drake Passage. The ACC has a multi-front structure, the two most prominent features being the Subantarctic Front and the Polar Front. Pratt (1989) has made estimates of the beta Froude number (6.4.13b) at the Drake Passage and at 134W section, upstream of the Passage. The value of ΔL^* is taken as the distance between the two fronts, whereas L_β is as the observed decay scale of the velocity away from the fronts and is given a range of values. As it turns out F_β ranges between 10^{-2} and 10^{-1} at the upstream section, and between .4 and .9 in the Drake Passage. This could be an indication of a hydraulic transition within the strait, but validation of this conjecture would require a more specific and sophisticated model.

The dependence of the model on the westward, far field velocity u_o results from the fact that the theory is purely inertial. If this far field flow is brought to zero, it can be shown (Exercise 3) that critical control is expunged. A more realistic far field in the ocean might be the wind-driven subtropical and subpolar gyres that exist between jets such as the Gulf Stream, but this would require the addition of forcing to the model.

Comparison of the quasigeostrophic, mid-latitude jet with the equatorial jet of the previous section yields some important similarities and differences. Critical control in each case involves a parameter $U/\beta^* L^2$ which must typically be O(1). However, there are differences in how U, β^*, and L are interpreted in the two cases. In the equatorial jet U is the typical velocity in the jet, β^* is its value on the equator, and L is the jet half width. As the flow passes over the ridge β^* remains constant while the velocity and width evolve in response to vortex squashing. In the mid-latitude jet, changes are forced by changes in the total ambient potential vorticity gradient and thus β^* is the sum of the planetary and topographic potential vorticity gradients. In addition, L is the inertial boundary layer thickness and U is a velocity scale based on the difference across the jet of the intrinsic potential vorticity. Another complication it that the true Froude number for the flow involves more than just a properly interpreted $U/\beta^* L^2$.

A common feature of the two models is that hydraulic behavior is reflected entirely in terms of *varicose* motions of the jet; that is, motions that effect the width. In the equatorial case, this is guaranteed by the assumption of the north-south symmetry that is integral to the similarity solution. In the mid-latitude jet, however, meandering (or *sinuous*) motions are present but are slaved to the varicose motions.

At the time of this writing, the potential hydraulic behavior of free, zonal jets had not received much attention or verification in observed or numerically modeled flows.

Exercises

1. Discuss the hydraulic control problem for a westward jet flowing over a northward sloping ridge.

2. Suppose that varicose motion of the jet is eliminated by taking the limit $\Delta L \to 0$. Show that the resulting meandering, cusped jet cannot undergo hydraulic transitions.

3. Explore the limit of a quiescent far field but taking the simultaneous limit $\beta \to 0$ and $u_o \to 0$ such that (u_o/β) remains constant. Show that no hydraulic transitions are possible.

Figure Captions

Figure 6.4.1 Definition sketch for a midlatitude jet with piecewise continuous potential vorticity distribution. (Based on Figure 1 of Pratt 1989).

Figure 6.4.2 The jet width ΔL *vs*. the northward slope parameter $s\mathcal{N}$ for $Q=\alpha=\beta=1$, a-c=8. Based on Equation 6.4.9. (Figure 2 of Pratt 1989)

Figure 6.4.3 Examples of the four solutions types based on the parameters of the previous figure, but with a-c=6.5, b-c=1, and $\mathcal{N} = \mathcal{N}_{\max} \exp(-x^2)$. $\mathcal{N}_{\max}$ has value .0164 (subcritical); .0622 (critically controlled); .0610 (supercritical); and .0622 (supercritical to subcritical). The flow is from left to right. (Figure 3 of Pratt 1989)

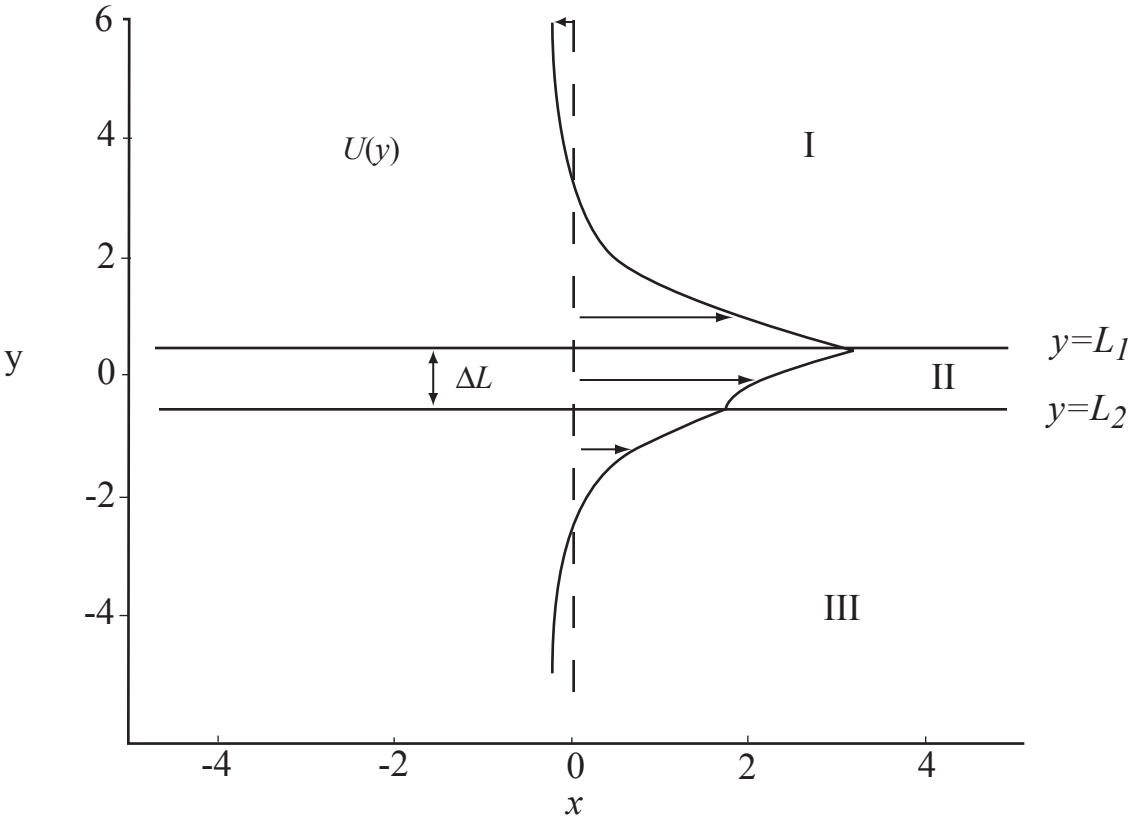

Figure 6.4.1

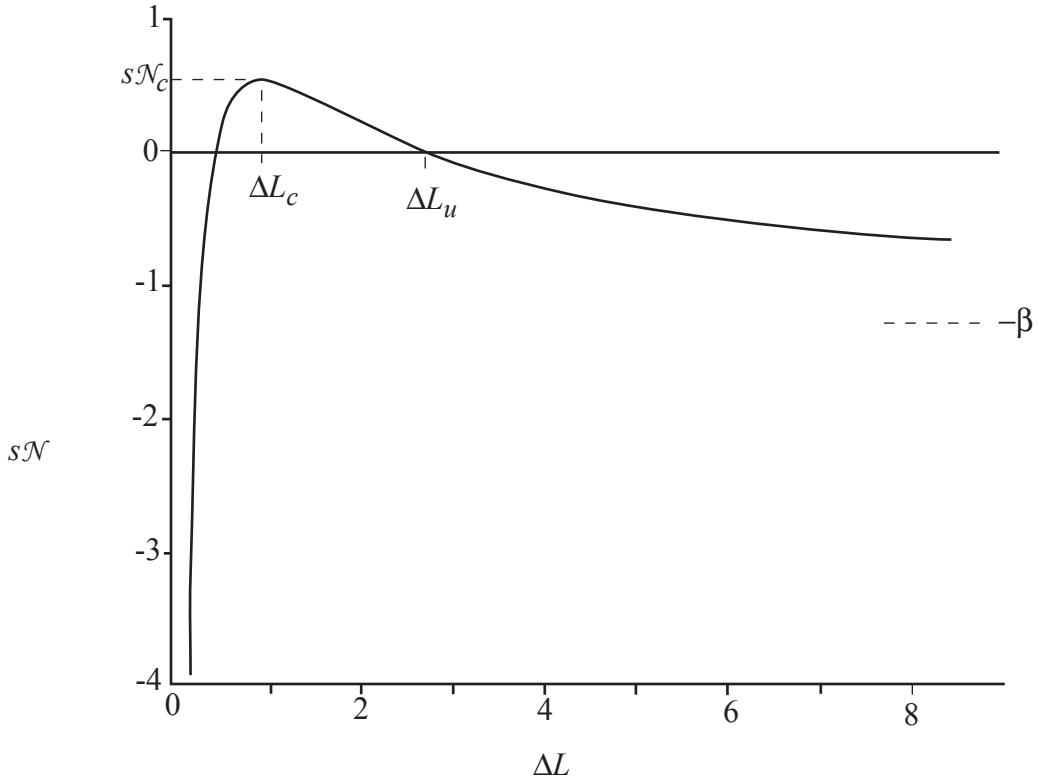
1
$s\mathcal{N}_c$
0
ΔL_c
ΔL_u
-1
$-\beta$
$s\mathcal{N}$
-2
-3
-4
0
2
4
6
8
ΔL

Figure 6.4.2

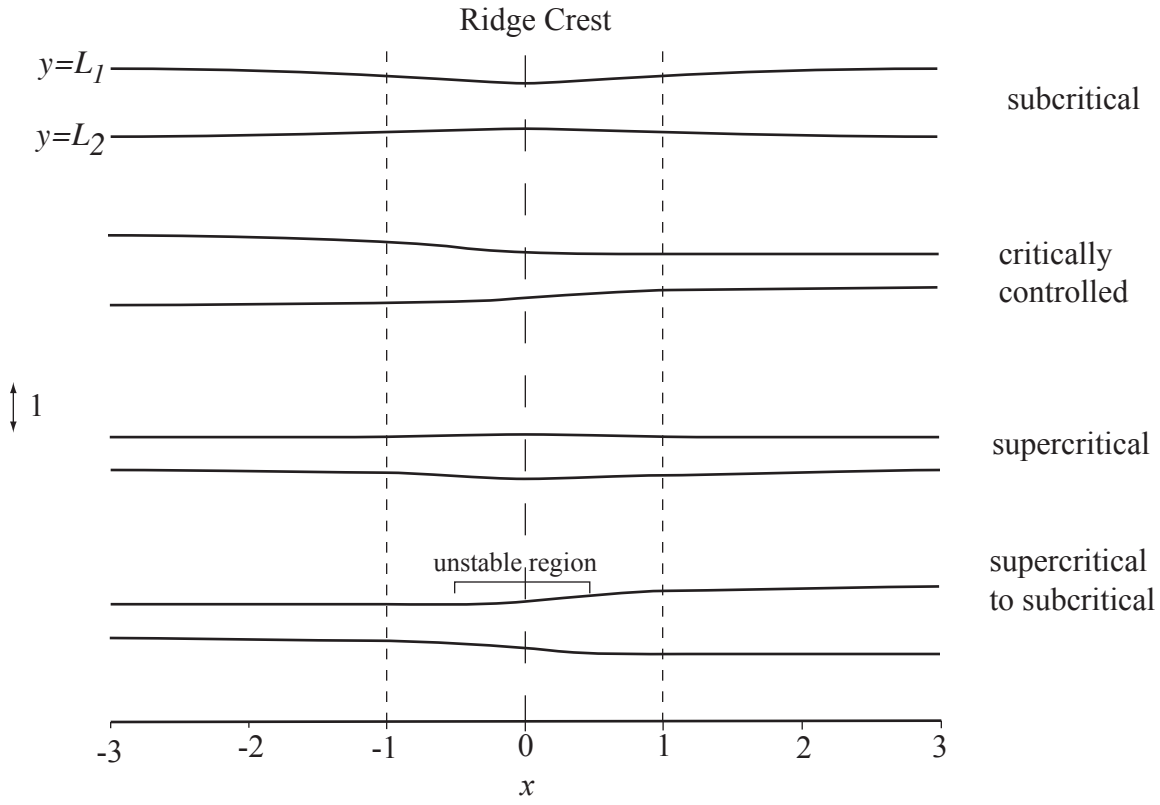
Ridge Crest
y=L1
y=L2
subcritical
critically
controlled
1
supercritical
unstable region
supercritical
to subcritical
-3
-2
-1
0
1
2
3
x

Figure 6.4.3